Journal of Macromolecular Science, Part A
Publication details, including instructions for authors and subscription information:
http://www.informaworld.com/smpp/title~content=t713597274

Polymer Compatibility by Continuous Thermodynamics

Margit T. Rätzsch[a]; Horst Kehlen[a]; Detlef Thieme[a]
[a] Chemistry Department, “Carl Schorlemmer” Technical University, German Democratic Republic

To cite this Article Rätzsch, Margit T. , Kehlen, Horst and Thieme, Detlef(1986) 'Polymer Compatibility by Continuous Thermodynamics', Journal of Macromolecular Science, Part A, 23: 7, 811 — 822

To link to this Article: DOI: 10.1080/00222338608069473

URL: http://dx.doi.org/10.1080/00222338608069473

J. MACROMOL. SCI.–CHEM., A23(7), pp. 811-822 (1986)

Polymer Compatibility by Continuous Thermodynamics

MARGIT T. RÄTZSCH, HORST KEHLEN, and DETLEF THIEME

Chemistry Department
"Carl Schorlemmer" Technical University
DDR-4200 Merseburg, German Democratic Republic

ABSTRACT

By applying a continuous distribution function instead of the mole fractions, mass fractions, etc. of individual components, continuous thermodynamics permits a drastic reduction of the computational expense for calculating phase equilibria in complex multicomponent systems such as petroleum fractions, shale oils, polymer solutions, and polymer mixtures. In this paper, continuous thermodynamics is applied to compatibility in mixtures of two polymers. If, e.g., the cloud-point curve is known, the shadow curve, the spinodal, the critical mixing point, and other interesting quantities may easily be calculated. Some examples are given to illustrate the method.

INTRODUCTION

Owing to the very large number of different species present, the characterization of the composition of synthetic polymers on the basis of the true polymer species is impractical. Thus, for thermodynamic treatment, either a number of neighboring species is united to form a pseudocomponent or a continuous distribution function may be used to describe the composition. The latter method, called continuous thermo-

0022-233X/86/2307-0811$3.50/0

dynamics, was established by Kehlen and Rätzsch [1] and later by Gualtieri et al. [2], Salacuse and Stell [3], and Briano and Glandt [4]. In comparison to the pseudocomponent method, the main advantages of continuous thermodynamics are a very compact mathematical description, a reduction of the computer time by a factor of approximately 30, and many fewer convergence problems.

Continuous thermodynamics is a useful method for all mixtures containing a large number of very similar chemical species. Application to the phase equilibria of systems with homopolymers or statistical copolymers has been presented by some of the present authors [5-7]. In this paper the problem of polymer compatibility in mixtures of two polymers will be dealt with.

PHASE EQUILIBRIUM

Consider a system of two polymers, B and C. In traditional thermodynamics the condition for equilibrium between two phases, ' and '', may be expressed by their chemical potentials in the well-known manner:

$$\mu_{B_i}{}' = \mu_{B_i}{}'',$$

$$\mu_{C_j}{}' = \mu_{C_j}{}''. \tag{1}$$

These relations must be valid for all individual species (or for all pseudocomponents) i of the Polymer B and correspondingly for all individual species (or for all pseudocomponents) j of the Polymer C.

In continuous thermodynamics the phase equilibrium condition reads

$$\mu_B{}'(M) = \mu_B{}''(M),$$

$$\mu_C{}'(N) = \mu_C{}''(N). \tag{2}$$

This means that the polymers are considered as continuous ensembles of species in the continuous treatment. Of course, the amount of each continuous species is infinitely small. The continuous species are characterized by a continuous variable M or N which may be the molar mass, the degree of polymerization, the number of segments, etc. (Of course, we may choose M = N, but we are not forced to do so.) Relations (2) must be valid for the total ranges of the M-values–from M_0 up to M^0–and N-values–N_0 up to N^0–, respectively.

To apply Relations (2), we need expressions for the continuous versions of the chemical potentials. These may be obtained from the corresponding expressions in traditional thermodynamics as shown previously [5, 6]. For Polymer B we obtain

$$\mu_B(M) = \mu_{B,0}{}^*(M,T,P) + RT\left[\ln \psi_B W_B(M) + 1 - \frac{r_B(M)}{\bar{r}_n}\right] + r_B(M)RT \ln \bar{\bar{\gamma}}_B(M). \tag{3}$$

The relation for Polymer C reads analogously; it may easily be obtained by replacing B by C and M by N.

In Eq. (3) the first term on the right-hand side is a standard potential independent of the composition. The second term is the well-known Flory-Huggins contribution. Here, ψ_B is the total segment fraction of Polymer B in the mixture, and $W_B(M)$ is the distribution function of this polymer. Its definition reads: $\psi_B W_B(M)dM$ is the segment fraction of all B-species with M-values between M and M + dM. Thus, the distribution function obeys the normalization condition

$$\int_{M_0}^{M^0} W_B(M)dM = 1. \tag{4}$$

The quantity $r_B(M)$ is the segment number of the species indicated, and $\bar{r}_{n,B}$ is the corresponding number average:

$$\frac{1}{\bar{r}_{n,B}} = \int_{M_0}^{M^0} \frac{W_B(M)}{r_B(M)}\, dM. \tag{5}$$

The third term in Eq. (3) containing the so-called segment molar activity coefficient $\bar{\bar{\gamma}}_B(M)$ describes the excess with respect to a Flory-Huggins mixture.

The quantities referring to Polymer C are defined analogously. The symbol $\bar{r}_n$ signifies the number-average segment number for the total mixture

$$\frac{1}{\bar{r}_n} = \frac{\psi_B}{\bar{r}_{n,B}} + \frac{\psi_C}{\bar{r}_{n,C}}; \qquad \psi_B + \psi_C = 1. \tag{6}$$

For applications, the segment molar activity coefficients $\bar{\bar{\gamma}}_B(M)$ and $\bar{\bar{\gamma}}_C(N)$ may be calculated by using current model theories such as Huggins' χ-parameter concept or the Flory-Orwoll-Vrij theory. In this paper a linear dependence of the Huggins' χ-parameter with respect to ψ_B and $1/T$ is assumed to follow

$$\bar{\bar{G}}^E/RT = \psi_B(1 - \psi_B)\chi = \psi_B(1 - \psi_B)(1 + c\psi_B)(a + b/T). \tag{7}$$

Here $\bar{\bar{G}}^E$ is the deviation of Gibbs energy from its value for a Flory-Huggins mixture considered for a mole of segments. Relation (7) contains three adjustable parameters a, b, c. It is a relatively simple expression because $\bar{\bar{G}}^E$ does not depend on the distribution functions $W_B(M)$ and $W_C(N)$. As long as we consider polymers and not oligomers, this independence is a good approximation. It results in the independence of $\bar{\bar{\gamma}}_B$ and $\bar{\bar{\gamma}}_C$ from M and N, respectively [5, 6], and we obtain

$$\ln \bar{\bar{\gamma}}_B = (1 - \psi_B)^2\ (1 + 2c\psi_B)(a + b/T),$$
$$\ln \bar{\bar{\gamma}}_C = \psi_B^{\ 2}(1 - c + 2c\psi_B)(a + b/T). \tag{8}$$

CLOUD-POINT CURVE AND SHADOW CURVE

In considering polymer compatibility, we are interested in the cloud-point curve and the shadow curve. The cloud-point curve describes the temperature of the beginning of phase separation as a function of the composition ψ_B' of a phase ' with given Polymers B and C characterized by their distribution functions $W_B'(M)$ and $W_C'(N)$. The shadow curve provides the composition ψ_B'' of the first droplets formed for the new phase ''.

Introducing Eq. (3) and the corresponding expression for Polymer C into the phase equilibrium condition (2), we obtain, after rearranging,

$$W_B''(M) = \frac{\psi_B'}{\psi_B''} W_B'(M) \exp [\rho_B r_B(M)], \tag{9}$$

with

$$\rho_B = \frac{1}{\bar{r}_n''} - \frac{1}{\bar{r}_n'} - \ln \bar{\bar{\gamma}}_B'' + \ln \bar{\bar{\gamma}}_B'. \tag{10}$$

The resulting expressions for $W_C''(N)$ and ρ_C read analogously. According to Eq. (4), integration leads to

$$\psi_B'' = \int_{M_0}^{M^0} \psi_B' W_B'(M) \exp\,[\rho_B r_B(M)]\,dM, \tag{11}$$

$$1 - \psi_B'' = \int_{N_0}^{N^0} (1 - \psi_B') W_C'(N) \exp\,[\rho_C r_C(N)]\,dN. \tag{12}$$

In these two equations, three unknowns occur: T, ψ_B'', and $\bar{r}_n''$. Thus, completing Eqs. (11) and (12) by the relation

$$\frac{1}{\bar{r}_n''} = \int_{M_0}^{M^0} \frac{\psi_B' W_B'(M)}{r_B(M)} \exp\,[\rho_B r_B(M)]\,dM + \int_{N_0}^{N^0} \frac{(1 - \psi_B') W_C'(N)}{r_C(N)} \exp\,[\rho_C r_C(N)]\,dN, \tag{13}$$

resulting from Eqs. (5) and (6), we obtain a system of three equations for the three unknown quantities. If T, ψ_B'', and $\bar{r}_n''$ are calculated in this way, the unknown distribution functions $W_B''(M)$ and $W_C''(N)$ are immediately given by Eq. (9) and the analogous relation for Polymer C.

In the general case, the integrals in Eqs. (11)-(13) must be calculated by numerical methods. But, on the assumption that Schulz-Flory distributions are suitable for describing the distribution functions in the given phase ', i.e., the expression

$$W_B'(r_B) = \frac{k_B^{\,k_B+1}}{\bar{r}_{n,B}'\,\Gamma(k_B + 1)} \left(\frac{r_B}{\bar{r}_{n,B}'}\right)^{k_B} \exp\left(-k_B \frac{r_B}{\bar{r}_{n,B}'}\right) \tag{14}$$

and an analogous relation for $W_C'(r_C)$ are applicable, all integrals occurring may be calculated analytically. In (14), we simply have chosen $M = r_B(M)$. The parameters of (14) are $\bar{r}_{n,B}'$ and k_B; Γ means the Γ-function. For this case, the analytical solution of the integrals in Eqs. (11)-(13) leads to the following expressions:

$$\psi_B'' = \psi_B' \left(1 - \frac{\bar{r}_{n,B}'\rho_B}{k_B}\right)^{-(k_B+1)}, \tag{15}$$

$$1 - \psi_B'' = (1 - \psi_B')\left(1 - \frac{\bar{r}_{n,C}'\rho_C}{k_C}\right)^{-(k_C+1)}, \tag{16}$$

$$\frac{1}{\bar{r}_n''} = \frac{\psi_B'}{\bar{r}_{n,B}'}\left(1 - \frac{\bar{r}_{n,B}'\rho_B}{k_B}\right)^{-k_B} + \frac{(1 - \psi_B')}{\bar{r}_{n,C}'}\left(1 - \frac{\bar{r}_{n,C}'\rho_C}{k_C}\right)^{-k_C}. \tag{17}$$

Relations (15)-(17) permit the elimination of $\bar{r}_n''$ and T. Thus, there remains only one (implicit) equation with the unknown ψ_B'' for numeric solution. Furthermore, the distribution functions in phase '' prove to be the Schulz-Flory distributions too.

SPINODAL AND CRITICAL POINT

If $\bar{\bar{G}}^E$ does not depend on the distribution functions $W_B(M)$ and $W_C(N)$, such as in Eq. (7), continuous thermodynamics leads to the following relation for the spinodal [8]:

$$\frac{1}{\psi_B\bar{r}_{w,B}} + \frac{1}{(1 - \psi_B)\bar{r}_{w,C}} + \left(\frac{\partial^2\bar{\bar{G}}^E/RT}{\partial\psi_B^2}\right)_{T,P} = 0. \tag{18}$$

The critical mixing point is characterized by the additional validity of the equation [8]:

$$-\frac{\bar{r}_{z,B}}{\psi_B^2 \bar{r}_{w,B}^2} + \frac{\bar{r}_{z,C}}{(1-\psi_B)^2 \bar{r}_{w,C}^2} + \left(\frac{\partial^3 \bar{G}^E/RT}{\partial \psi_B^3}\right)_{T,P} = 0. \qquad (19)$$

In Eqs. (18) and (19), $\bar{r}_w$ and $\bar{r}_z$ indicate the weight-average and the z-average. Relations (18) and (19) have also been extablished on the basis of traditional thermodynamics [9].

EXAMPLES

As examples, we will consider some polymer blends known from the literature [10-13]: three different systems of polystyrene + poly(vinyl methyl ether) (Figs. 1-3) showing lower critical solution tem-

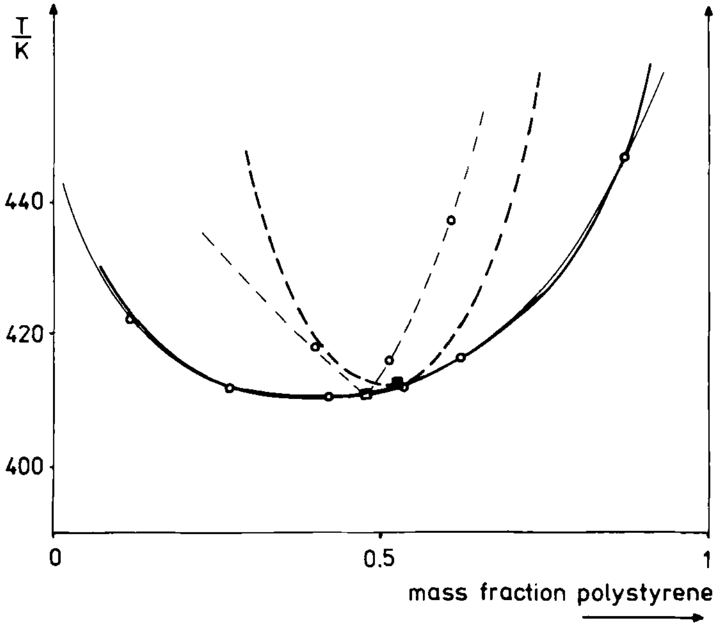

FIG. 1. A polystyrene + poly(vinyl methyl ether) blend: Experimental cloud points (—o—) and fitted cloud-point curve (—). Comparison of experimental (--o--) and predicted (--) spinodal and of experimental (□) and predicted (■) critical point.

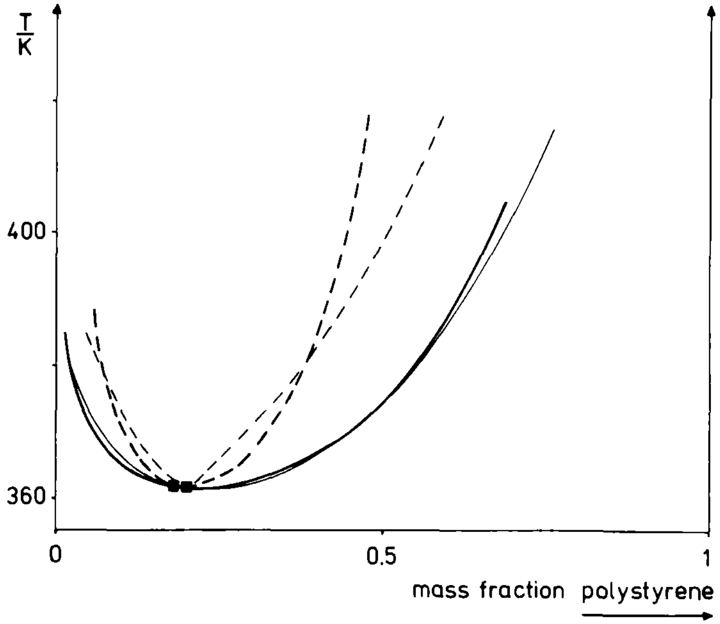

FIG. 2. A polystyrene + poly(vinyl methyl ether) blend: Experimental (——) and fitted (——) cloud-point curve. Comparison of experimental line of demarcation between phase separation morphologies (– –) and predicted spinodal (– –) and of experimental (□) and predicted (■) critical point.

perature behavior and one system of polystyrene + poly(methylphenylsiloxane) (Fig. 4) with an upper critical solution temperature. In all cases the polymers can be characterized by Schulz-Flory distributions, leading to the applicability of the simpler formulas (15)-(17). The Schulz-Flory parameters $\overline{r}_n$ and k for the polymers are listed in Table 1, together with the parameters a, b, c introduced by the $\overline{\overline{G}}^E$-expression (Eq. 7). The latter parameters were obtained by fitting to the experimental cloud-point curve data. The good reproduction of the experimental cloud points by the calculated curve shows the applicability of the model Expression (7) for $\overline{\overline{G}}^E$.

In the case of Fig. 1, Synder and Meakin [10] published not only experimental cloud points but also experimental spinodal data. Hence, the predicted spinodal curve and the predicted critical point can be compared to experimental data. Figure 1 shows that the experimental values are well predicted.

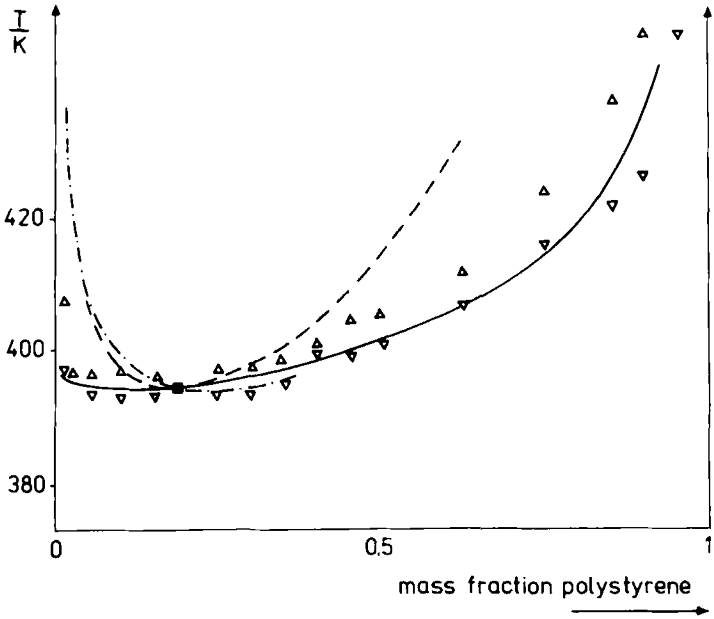

FIG. 3. A polystyrene + poly(vinyl methyl ether) blend: Experimental cloud points (△, heating; ▽, cooling) and fitted cloud-point curve (—). Predicted shadow curve (- ·), predicted spinodal (- -), and predicted critical point (■).

For the system of Fig. 2, Nishi, Wang, and Kwei [11] reported, in addition to the experimental cloud points, experimental data on the line of demarcation between phase separation morphologies. As this line should be very near the spinodal, a comparison analogous to that in Fig. 1 shows a good prediction of the experimental data.

McMaster [12] (Fig. 3) gives experimental data only on the cloud-point curve. Hence, no comparison between experimental and predicted data is possible. Here, the predicted shadow curve is also plotted.

Nearly the same holds in the case of Fig. 4 based on data by Nojima and Nose [13]. The predicted shadow curve and the predicted spinodal were plotted. The only experimental information permitting a comparison between experiment and prediction is the critical point, but in this case the agreement is not as good as in Figs. 1 and 2.

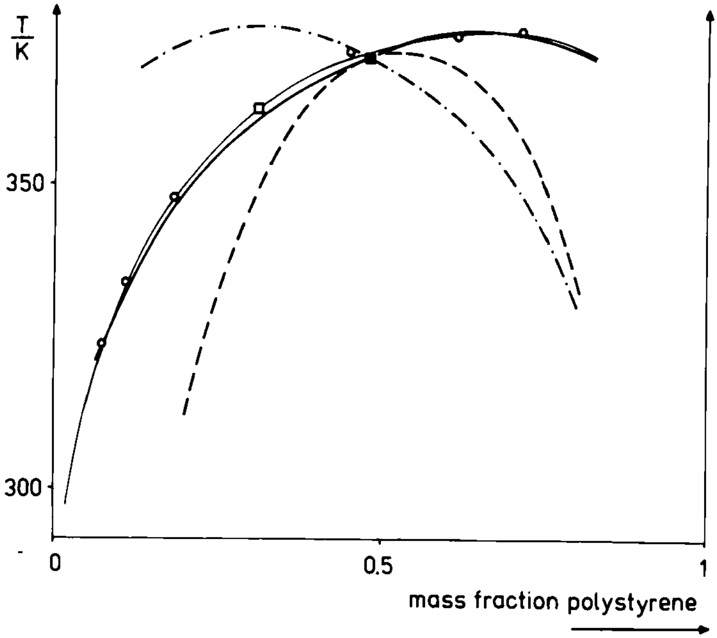

FIG. 4. A polystyrene + poly(methylphenylsiloxane) blend: Experimental cloud points (—○—) and fitted cloud-point curve (—). Predicted shadow curve (—·) and predicted spinodal (– –). Comparison of experimental (□) and predicted (■) critical point.

TABLE 1. Parameters $\bar{r}_n$ and k of the Schulz-Flory Distributions Characterizing the Polymers Considered and Parameters a, b, c of the $\bar{\bar{G}}^E$ Model Applied

Fig.	System	Ref.	$\bar{r}_n M_S$*	k	$\frac{a}{10^{-4} M_S}$	$\frac{b/K}{M_S}$	c
1	Polystyrene +	10	15 000	0.33	1.2353	-0.0375	0‡
	poly(vinyl methyl ether)		35 900	1.34			
2	Polystyrene +	11	200 000	16.7	1.5503	-0.04955	-0.836
	poly(vinyl methyl ether)		25 750	1†			
3	Polystyrene +	12	78 000	0.49	6.5591	-0.23756	-0.111
	poly(vinyl methyl ether)		7 700	1.37			
4	Polystyrene +	13	8 490	16.7	-11.589	0.56523	0.577
	poly(methylphenylsiloxane)		1 780	1.75			

*M_S is the molar mass of a segment. Because we have chosen $M_{S,B} = M_{S,C} = M_S$, there is no need to specify M_S.

†k is assumed to equal 1 because no value was published.

‡Because the fitted value approximately equals zero, the calculations were performed with c = 0.

REFERENCES

[1] H. Kehlen and M. T. Rätzsch, Proceedings of the 6th International Conference on Thermodynamics, Merseburg, 1980, p. 41.

[2] J. A. Gualtieri, J. M. Kincaid, and G. Morrison, J. Chem. Phys., 77, 521 (1982).

[3] J. J. Salacuse and G. Stell, Ibid., 77, 3714 (1982).

[4] J. G. Briano and E. D. Glandt, Fluid Phase Equilibria, 14, 91 (1983).

[5] H. Kehlen and M. T. Rätzsch, Z. Phys. Chem. (Leipzig), 264, 1153 (1983).

[6] M. T. Rätzsch and H. Kehlen, J. Macromol. Sci.–Chem., A22, 323 (1985).

[7] M. T. Rätzsch, H. Kehlen, and D. Browarzik, Ibid., A22, 1679 (1985).

[8] J. Bergmann, H. Kehlen, and M. T. Rätzsch, Z. Angew. Math. Mech., 65, 343 (1985).

[9] R. Koningsveld, L. A. Kleintjens, and H. M. Schoffeleers, Pure Appl. Chem., 39, 1 (1974).

[10] H. L. Snyder and P. Meakin, Polym. Prepr., 24, 411 (1983).

[11] T. Nishi, T. T. Wang, and T. K. Kwei, Macromolecules, 8, 227 (1975).

[12] L. P. McMaster, Ibid., 6, 760 (1973).

[13] S. Nojima and T. Nose, Polym. J., 14, 269 (1983).

Received April 13, 1985